ELSEVIER

Journal of Applied Geophysics 45 (2000) 225–237

JOURNAL OF APPLIED GEOPHYSICS

www.elsevier.nl/locate/jappgeo

Recent advances in seismic monitoring technology at Canadian mines

Theodore I. Urbancic *, Cezar-Ioan Trifu

Engineering Seismology Group Canada, 1 Hyperion Ct., Kingston, Ontario, Canada K7K 7G3

Received 23 April 1999; accepted 14 September 2000

Abstract

We provide an overview of the current status of seismic monitoring instrumentation employed in Canadian underground mines. Based on several case studies, we outline how passive seismic monitoring techniques are being used to evaluate fractures and stress conditions associated with ore extraction at depth. It is shown that induced microseismicity allows for the remote monitoring of active fractures, delineating modes of failure with advancing excavation fronts, and identifying variations in principal stress orientations during sequential stages of mining. Advances into the characterization of excavation zone of influence through deformation state analysis and the use of seismic hazard analysis to evaluate the potential for ground instability are also discussed.

Keywords: Seismic monitoring; Microseismicity; Canadian mines

1. Introduction

Mining-induced seismicity is directly related to the interaction of mine excavations and geological structures with regional and local stress fields. Seismic energy is released when a frictional instability occurs on pre-existing geological structures, or when new fractures are formed. This has, in extreme circumstances, taken the form of rockbursts, which can potentially affect personal safety and mine integrity. As mining continues to greater depths in the future, the impact of rockbursts may have substantial economical implications. Therefore, understanding the mechanics of rockburst occurrence is critical for the design of effective and efficient mining operations.

Over the last decade, impressive progress in this area of study has occurred primarily as a result of advances in seismic instrumentation. The transition to digital high frequency full waveform data acquisition systems with increased dynamic range, has allowed for the monitoring of microseismicity in addition to rockbursts. As such, microseismic events, which are defined as events with magnitudes less than zero and comprise the largest percentage of seismic observations at a mine site, can now be used to provide information on the mechanics of strain energy accumulation due to mining and the changing rock mass conditions leading to the generation of rockbursts (Board, 1994).

* Corresponding author.
E-mail address: urbancic@esg.ca (T.I. Urbancic).

0926-9851/00/$ - see front matter
PII: S0926-9851(00)00030-6

The availability of waveform records has resulted in the application of several techniques traditionally employed in earthquakes studies, which provided insight into the failure mechanism, including possible fracture and stress orientations, and characteristics of the source, such as source strength, the extent of slip, energy and stress release. As a result, a better understanding of seismic source inhomogeneity (McGarr, 1991) and source scaling behaviour (Gibowicz, 1995) as related to mining has been achieved.

In this paper, we illustrate the development of seismic instrumentation and how seismological techniques have been used in Canadian mines over the past few years in order to characterize the rock mass conditions in the presence of excavations. Several

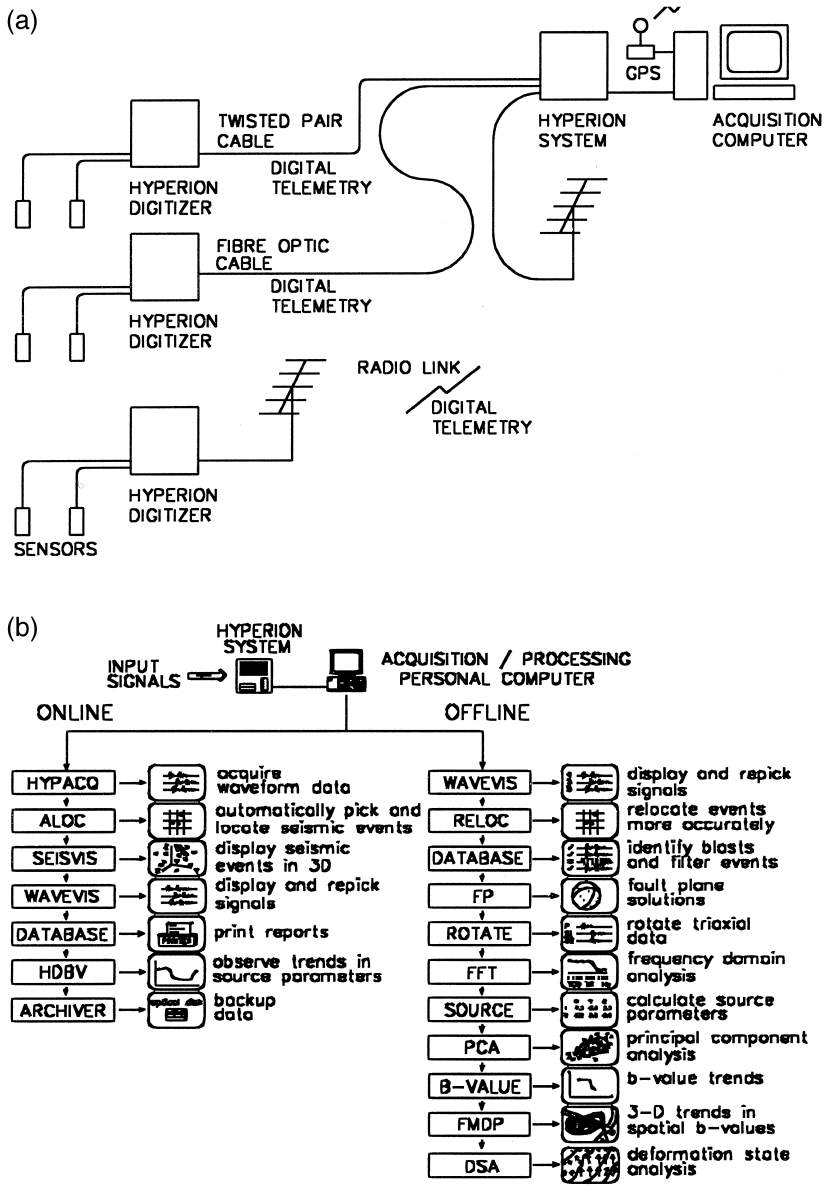

Fig. 1. Schematic diagrams of seismic monitoring (a) instrumentation and (b) software.

case studies are presented on how these techniques have been employed to map active structures, identify modes of failure with advancing mining, and characterize stress variations during sequential stages of excavation. Furthermore, we outline how microseismicity can be used to determine the extent of excavation influence and assess the seismic hazard associated with underground mining operations.

2. Instrumentation

In the past few years, advances in off-the-shelf hardware and software components have stimulated the development of readily available, reliable, and cost effective full-waveform seismic monitoring equipment. Moreover, on-line seismic analysis routines have provided mines with the capability to record and process event occurrence rates that may exceed 100 events per day. As such, seismology has become an accessible tool for remote on-going characterization of rock mass conditions under the influence of mining. Further, the installation and operation of seismic monitoring equipment have as a result been widely embraced by the mining community.

As shown in Fig. 1a, seismic monitoring installations are typically configured using twisted pair cable, fiber optics, radio telemetry, or a hybrid combination of the above. Digitization rates are up to 40 kHz with 16-bit resolution, allowing for the effective recording of events with magnitudes down to -3. Acquisition units employ complex trigger logic to reduce mis-triggers due to mine noise. Installed sensors are typically either uniaxial or triaxial accelerometers; however, geophones are commonly used for surface installations. A Global Positioning System (GPS) is employed to time-link regional and local systems.

Fig. 1b illustrates, as an example, software for data acquisition and processing of mine induced seismicity. The software operates in a multi-tasking environment, such as Microsoft Windows '98, enabling various applications to run concurrently. Seismic parameters are stored in database structures, allowing for advanced filtering of records based on user defined time, space and other parameter constraints. Data visualization and plotting routines are also available for 3-D viewing of seismicity and source parameters in real-time.

3. Identification of active structures

In underground mines, geological structures of varying size can be activated by the presence of workings and their interaction with the local/regional stress fields. The location of these fractures is provided by the spatial distribution of seismic events. By assuming that shear is the dominant mode of failure, it is possible to use seismic waveform information, such as compressional wave (P-wave) first motions, to also define possible orientations of active fractures (fault-plane solutions). The effectiveness of using the above approaches as a mapping tool can then be examined in the context of known geological structures (Urbancic et al., 1993).

In Fig. 2a, the distribution of poles to fractures is contoured on lower hemisphere equal area stereonets, as determined from underground mapping at Strathcona mine, Sudbury, Canada. The spatial clustering of event locations suggests that the events tended to preferentially align themselves along one of the mapped structural sets (Set A; Fig. 2b). This orientation is one of two outlined by using fault-plane solutions (Fig. 2c), and corresponds to the orientation obtained by assuming that these failures occurred under a single, relatively stable regional stress field (Fig. 2d). Based on these observations, it is clear that mining induced microseismicity is associated with pre-existing fractures, and that seismic analysis provides the means to remotely monitor active fractures throughout the mine.

4. Mechanisms of failure ahead of advancing mining fronts

The energy partition between the P-waves and shear (S-) waves can be used to evaluate the proportion of shear to non-shear components of failure

present in the seismic sources. Typically, the seismic energy release for P-waves is 20 to 30 times smaller than that for S-waves (Boatwright and Fletcher, 1984). Conversely, the P-wave and S-wave energy release are approximately equal for tensile failure (Sato, 1978). As a result, by examining the energy

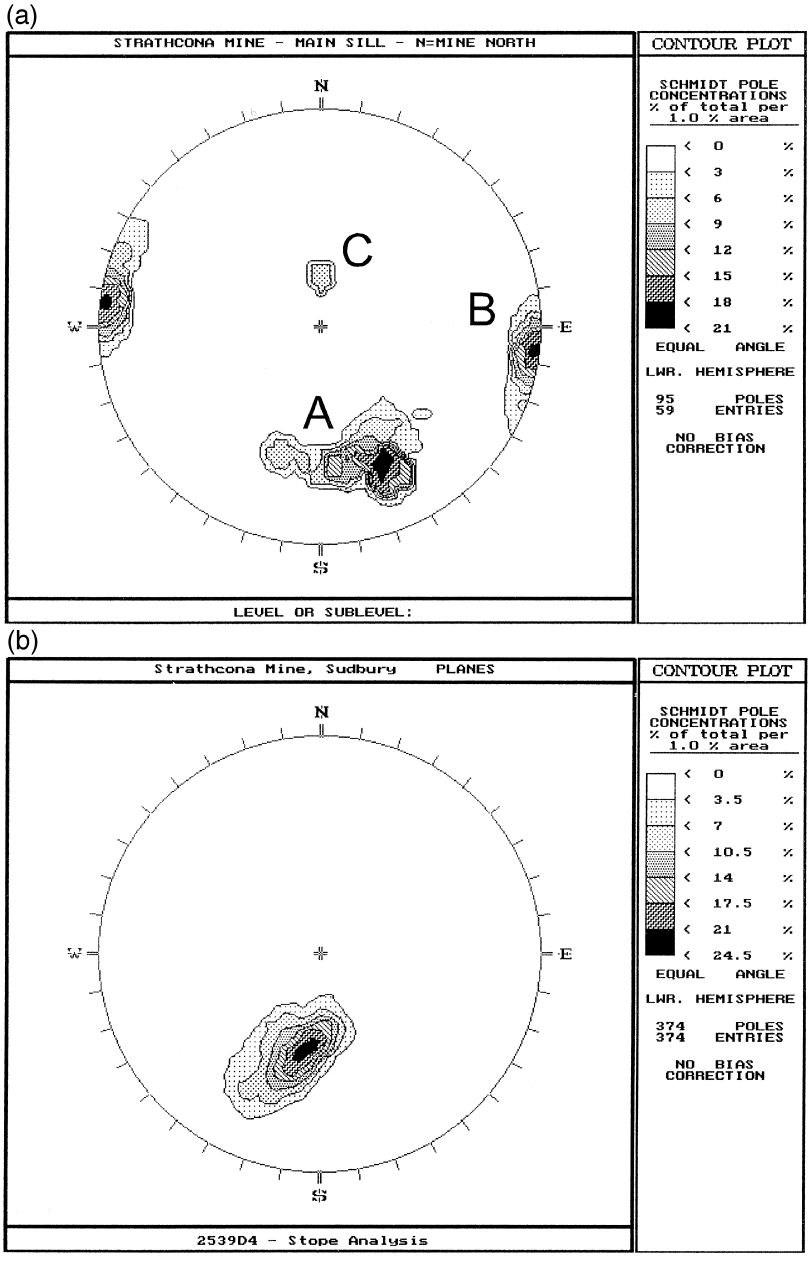

Fig. 2. Stereonet projections for Strathcona mine of the poles to the (a) mapped fractures, (b) spatial orientation of seismicity, (c) fault-plane solutions, (d) and stress field derived failure planes.

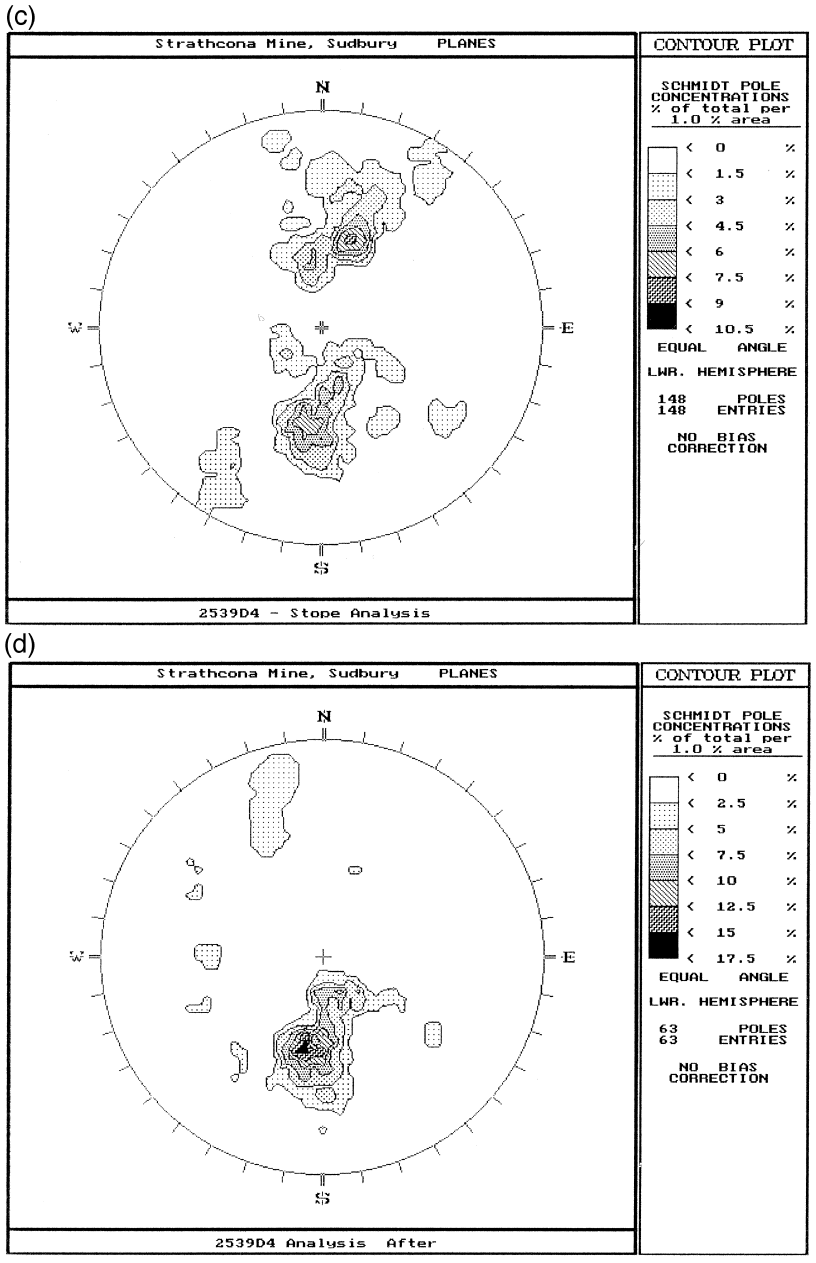

Fig. 2 (*continued*).

ratio it may be possible to evaluate the types of failures occurring with progressive mining (Urbancic and Young, 1993).

In Fig. 3, the energy values vary strongly with position relative to an advancing excavation face at Strathcona mine. The largest total seismic energy release occurred within 20 m of the excavation face, and within 20 m of its base. Both the P- and S-wave energies mirror the observed total energy distribution. The energy levels define three zones ahead of the excavation and two zones in depth. In Fig. 3b, events close to the excavation are enriched in P-wave

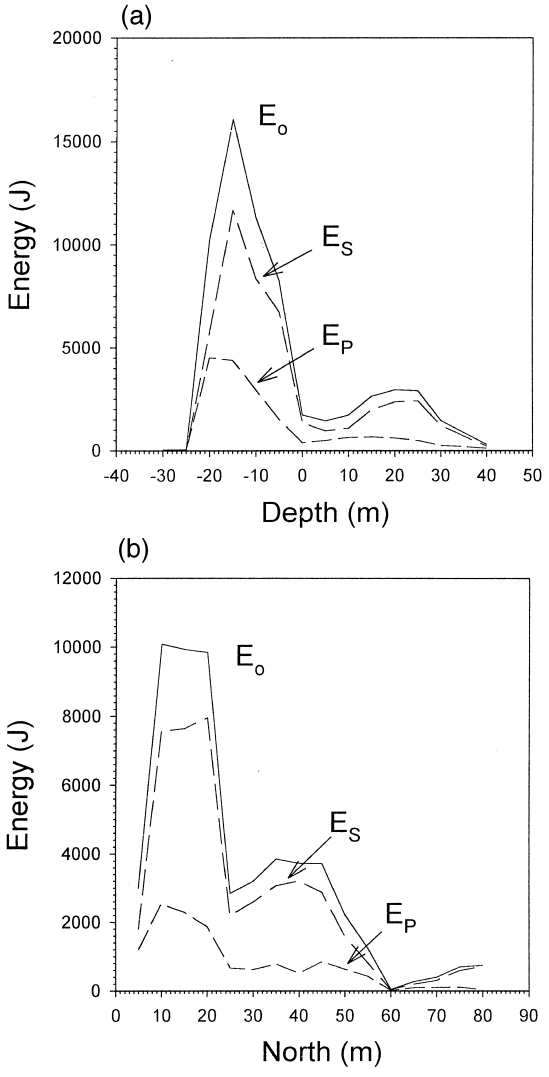

Fig. 3. Average total seismic energy (E_O), P-wave energy (E_P), and S-wave energy (E_S) values based on a 5-m moving window as a function of (a) depth above the excavation base and (b) ahead of the advancing excavation front (north).

energy, suggesting that a large non-shear failure component exists, whereas events at distance from the excavation face appear to be enriched in S-wave relative to P-wave energy implying the presence of a dominant shear failure mechanism. Between these two extremes exists a transition zone where failures have varying proportions of shear and non-shear components.

Based on fault-plane solutions, different fracture sets were activated in the three zones (Sets C, B, and A, respectively; Fig. 2), defining a systematic pattern of fracture behaviour with advancing excavation. By accounting for the potential effects these features may have on continued mining in highly stressed rock masses at depth, it is expected that on-going mine design extraction methodologies could be further improved.

5. Stress changes associated with mining sequences

In addition to defining the likely active fractures, fault-plane solutions provide information on the principal strain axes under which slip occurred. These axes are referred to as the pressure (P), null (B), and tension (T) axes, and under certain conditions they can be directly related to the principal stress axes. To define variations in stress during several stages of a mining sequence, a stress inversion technique can be employed, based on the principal strains, by assuming that at every stage of the sequence, the events occurred under a relatively stable stress field (Gephart and Forsyth, 1984).

From the analysis of microseismicity associated with five stages of a panel extraction within a sill pillar at 1050 m depth in Lockerby mine, Sudbury, Canada, two types of events were observed, (1) reverse faulting events within the sill and just below the sill (Fig. 4a) and (2) normal faulting events at the top of the sill (Fig. 4b). The principal stresses of the reverse faulting events for the five excavation stages in the sill remained relatively stable over the entire sequence (Fig. 4c), namely for three blasting intervals and during the pre/post-mining periods, with σ_1 approximately sub-horizontal and trending north–south, σ_2 sub-horizontal and trending east–west, and σ_3 sub-vertical. This trend of σ_1 differs by approximately 90° from that determined for the regional σ_1, trending east–west (Sampson-Forsyth, 1994). For the cluster below the sill, there is no change in the orientation of the induced stress field from the regional field. As with the reverse faulting, the stress field responsible for the normal faulting was found to be relatively stable over the entire study period (Fig. 4d), with σ_1 approximately sub-

vertical, σ_2 sub-horizontal and trending north–south, σ_3 sub-horizontal and trending east–west. This approach allows for the remote characterization of the dynamic behaviour of fractures based on the identified stress field within the rock mass. As such, for fractures activated under quasi-stable stress conditions, this methodology further assists in mine extraction strategies.

6. Delineation of the excavation zone of influence

Focal mechanism data, contained within limited volumes throughout a seismically active region, can be used to determine the rate of deformation associated with underground excavations. The method applies nearest neighbourhood statistics to individual *P* and *T* axes, and assumes that the deformation in the

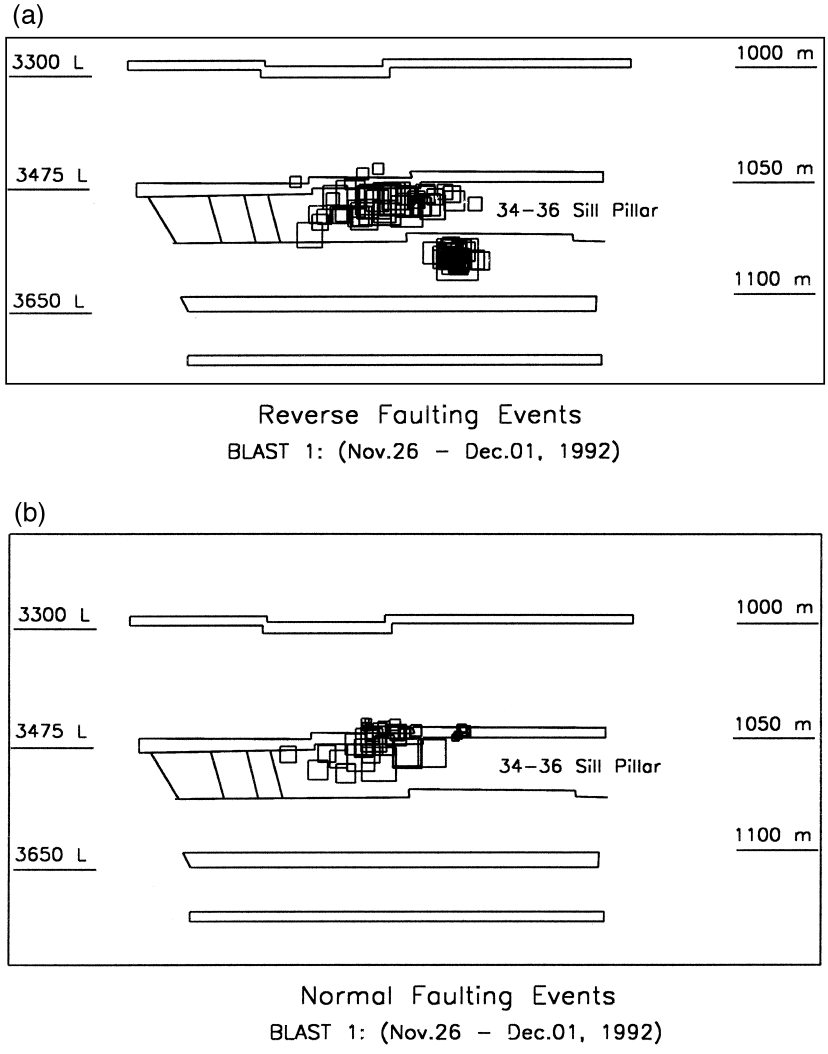

Fig. 4. Longitudinal view (looking north) showing the distribution of (a) reverse and (b) normal faulting events for the first blast interval. Principal stress axes (σ_1—open circles, σ_2—stars, σ_3—filled circles) of the reverse (c) and normal (d) faulting events for the different extraction stages: pre-mining (Pre), blast 1 (B1a for events within the sill and B1b for those below), blast 2 (B2), blast 3 (B3), and post-mining (Pst).

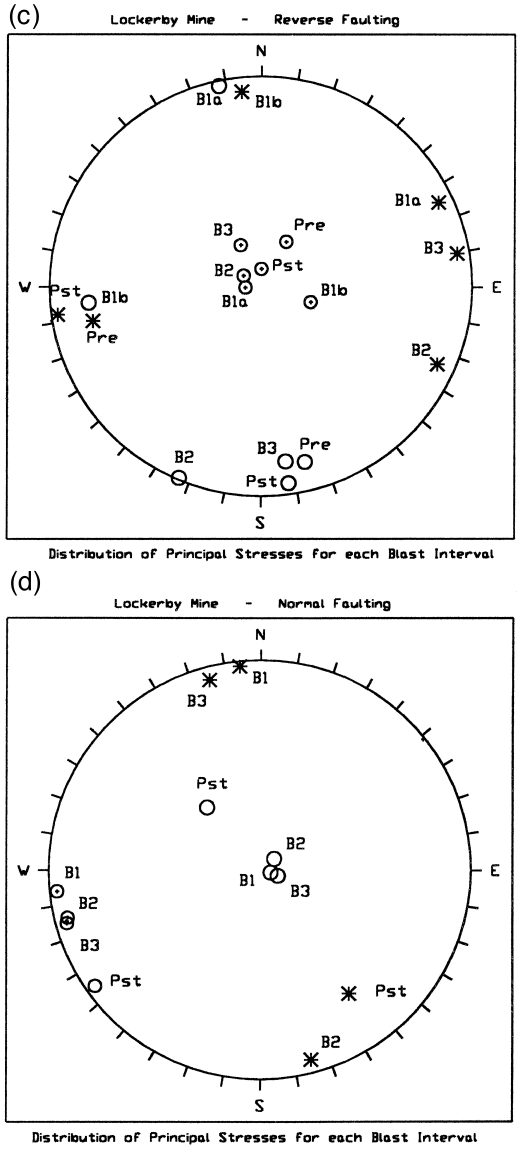

Fig. 4 (*continued*).

study volume acts similarly over the entire range of observed magnitudes (Kostrov and Das, 1988). To illustrate the potential of using deformation rate analysis to outline the extent of excavation influence on the surrounding rock mass, the method was applied to microseismicity recorded following two production blasts (stages 3 and 6; Fig. 5) of a sill pillar at about 900 m depth in Campbell mine, Balmertown, Canada (Urbancic et al., 1997).

In Fig. 6, the depth component of deformation rate is presented for both extraction stages. Following stage 3, the largest deformation rates, as expected, occurred in the excavation volume. However,

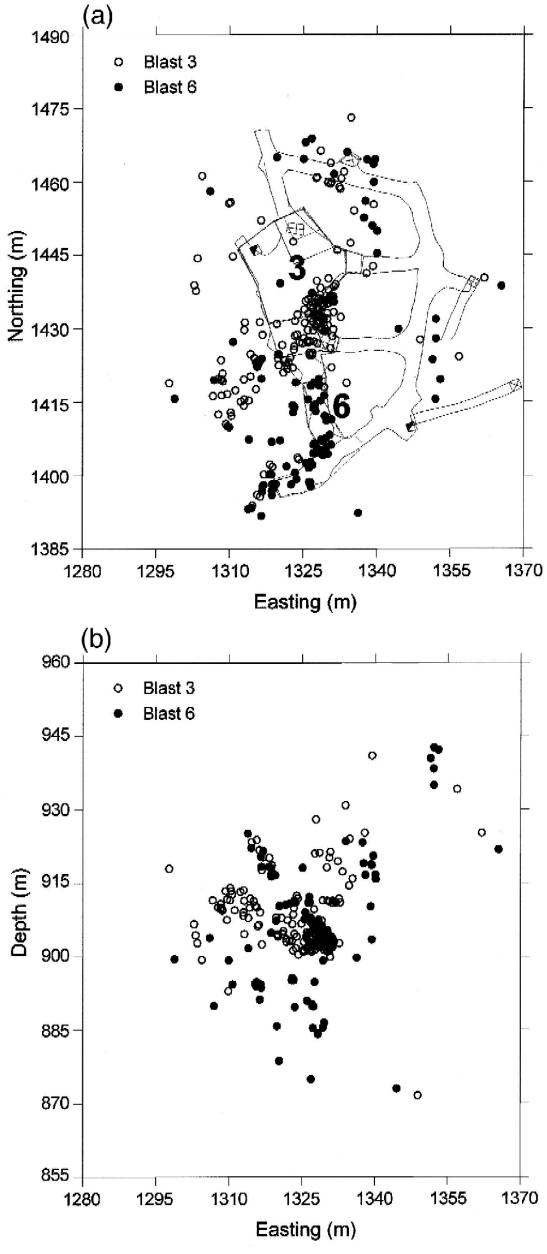

Fig. 5. Distribution of seismicity in plan view at (a) mid-sill height and (b) in cross-section for excavation stages 3 (open circles) and 6 (solid circles).

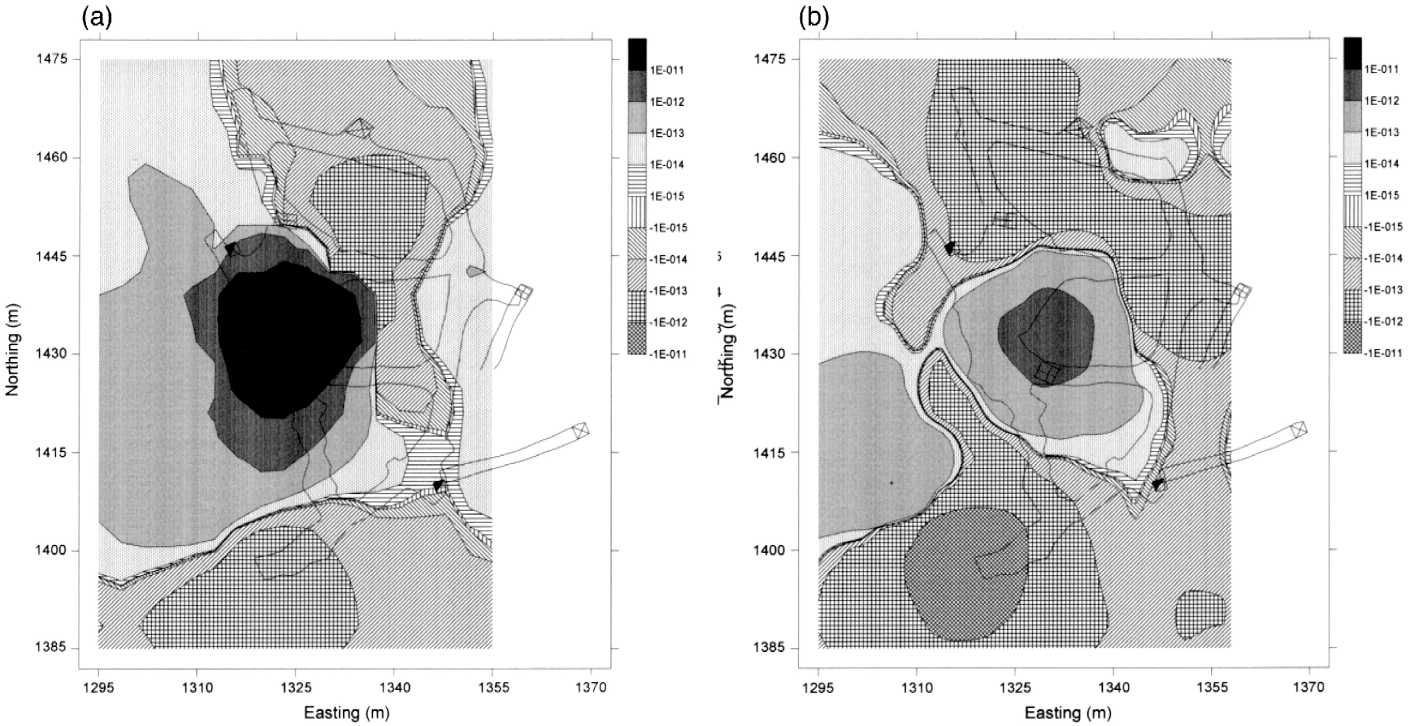

Fig. 6. Vertical deformation rate in day^{-1} for excavation stage 3 at (a) mid-sill height and (b) below the sill, and for excavation stage 6 at (c) mid-sill height and (d) below the sill.

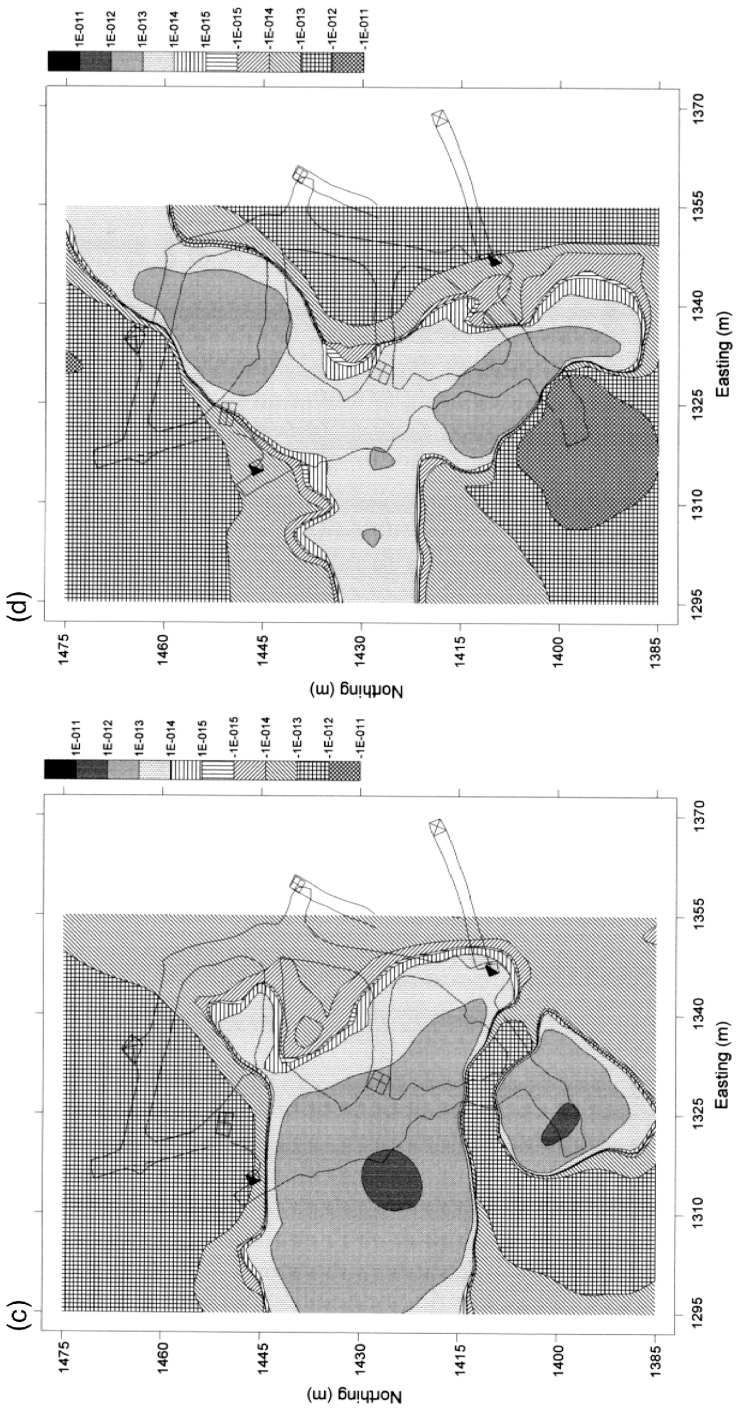

Fig. 6 (*continued*).

high rates were also observed outside the excavation, suggesting that the rock mass in the vicinity of the subsequent stage 6 excavation was already in a state of transformation. Similarly, following stage 6, high deformation rates were observed not only throughout the entire excavated volume, but also in the region of the subsequent stage 7 excavation. Interestingly, following stage 7, a ground fall occurred 15 m west and parallel to the long wall of stage 6, suggesting that there may be a link between the observed deformation rate and the occurrence of the ground fall. Future studies will be required to quantitatively establish a relationship between deformation rates and actual strain rates within the rock mass.

7. Seismic hazard assessment

The evaluation of seismic hazard is based on estimating the probability of exceeding critical peak velocity or acceleration values over time. To meet this goal, several parameters have to be determined, including the expected maximum magnitude levels, failure mechanisms, and effect of attenuation on signals transmitted to various sensor sites underground. One approach for evaluating the maximum magnitude levels is to examine the number-size event distribution in space and time. This can be achieved by combining both non-parametric and parametric statistics, based on nearest neighbourhoods (Trifu and Shumila, 1996), in order to calculate event occurrence rates at given magnitudes and the slope of the number-size distribution (*b*-value).

To test the appropriateness of evaluating space–time variations in *b*-value for the purposes of seismic hazard assessment, the above approach was applied to a catalogue of microseismic events recorded at depth (below 600 m) within Strathcona mine, Sudbury, Canada, for 1 month prior to and 1 month following a moment magnitude 2.9 rockburst. Fig. 7 shows the space–time distribution of *b*-values in the northing direction. As seen, the magnitude 2.9 rockburst, which occurred at day 28, was preceded by a decrease in the *b*-value from 1.2–1.4 to 0.6–0.8 over a period of about 2–3 days. Similar results were obtained when using either easting or depth as a space co-ordinate. The relative errors in the evaluation of *b*-values were found to be about 10–15%.

Based on these observations, the decrease in *b*-value prior to the occurrence of a large magnitude earthquake is likely associated with a relative increase in the effective stress (see Trifu and Urbancic, 1996). Under increasing stress conditions, there is a tendency for the higher strength areas to fail, leading to an increase of the microseismic activity at rela-

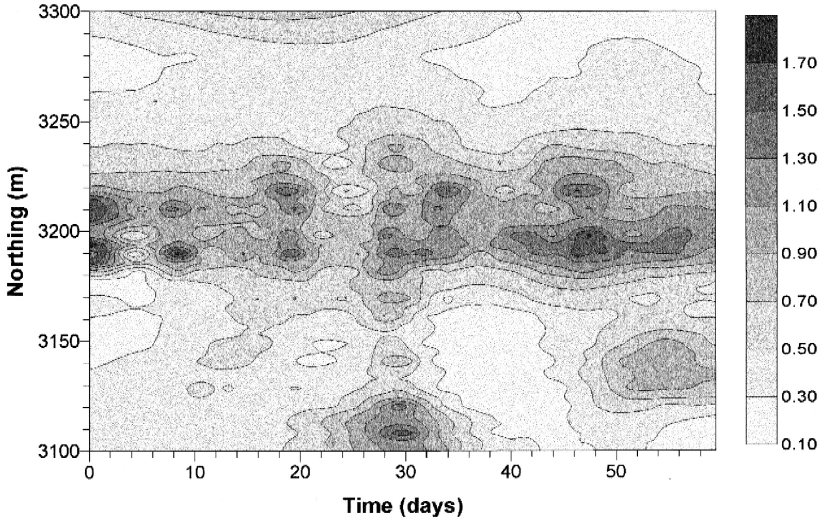

Fig. 7. Space–time distribution in northing of the *b*-values as calculated on a 5-m, 12-h grid.

tively higher magnitudes. Since the method has the advantage of allowing for the estimation of the seismicity parameters at every moment of time and each spatial location, it has the potential to be used to establish seismic hazard assessment maps in mines.

8. Conclusions

In the last decade, insight into mining induced seismicity, including the generation of rockbursts, has been expanded primarily through the development of high frequency data acquisition instrumentation with increased dynamic range, and the adaptation of earthquake analysis techniques to this environment. This has allowed for smaller events, with magnitudes less than zero, to be routinely recorded and processed in mines. As a result, a better understanding of the interaction between excavations, the regional stress field, and local structural geology has been achieved.

In this paper, we have provided examples of how different seismic techniques can be used at mine sites. These techniques include the identification of: (1) active fractures through the use of space–time distribution in microseismicity and fault-plane solutions; (2) mode of failure with respect to the excavation front by employing S- to P-wave energy ratios; and (3) local principal stress orientations in the vicinity of openings using stress inversion of principal strain axes. Applications of these studies to mining operations range from on-going design of blast and extraction procedures to defining support requirements.

The dilemma faced by mine operators is how to effectively and efficiently extract ore without jeopardizing safety. Issues such as ore zone delineation, defining the extent of excavation influence for dilution purposes, and identifying regions of potential instability are among the concerns that need to be addressed. As outlined, recent advances in seismic monitoring offer an opportunity to estimate the deformation and relative stress state of the rock mass in the presence of excavations, as well as the potential for evaluating the hazard associated with ground instability in mines.

Acknowledgements

This contribution incorporates results obtained from a series of studies funded by the Canadian Rockburst Research Project of the Canadian Mining Industry Research Organization (CAMIRO). We thank Falconbridge and Placer Dome for their assistance during the installation and operation of the microseismic instrumentation at their mines, and valuable discussions over the duration of the various projects. In particular, we would like to thank Graham Swan, Ian Clegg, and Bill Bromell at Strathcona mine, and Peter Mah, Drew Anwyll, Michel Gauthier at Campbell mine. We are also grateful to Mark Board and George Gibowicz for their suggestions on the original manuscript.

References

Board, M.P., 1994. Numerical examination of mining-induced seismicity. PhD Thesis, University of Minnesota, Minneapolis, MN, 240 pp.

Boatwright, J., Fletcher, J.B., 1984. The partition of radiated energy between *P* and *S* waves. Bull. Seismol. Soc. Am. 74, 361–376.

Gephart, J.W., Forsyth, D.W., 1984. An improved method for determining the regional stress tensor using earthquake focal mechanism data: Application to the San Fernando earthquake sequence. J. Geophys. Res. 89, 9305–9320.

Gibowicz, S.J., 1995. Scaling relations for seismic events induced by mining. Pure Appl. Geophys. 144, 191–209.

Kostrov, B.V., Das, S., 1988. Principles of Earthquake Source Mechanics. Cambridge Univ. Press, Cambridge.

McGarr, A., 1991. Observations constraining near-source ground motion estimated from locally recorded seismograms. J. Geophys. Res. 96, 16495–16508.

Sampson-Forsyth, A., 1994. Focal mechanisms of mining-induced microseismic events: their interpretation to prominent geological features and principal stress orientations in the 34–36 sill pillar at Falconbridge's Lockerby mine. MSc Thesis, Department of Mining Engineering, Queen's University, Kingston, Ontario.

Sato, T., 1978. A note on body wave radiation from expanding tension crack. Sci. Rep. Tohuku Univ., Ser. 5 25, 1–10.

Trifu, C.-I., Shumila, V.I., 1996. A statistically based space–time analysis of earthquake frequency-magnitude distribution with an application to the Vrancea region of Romania. Tectonophysics 216, 9–22.

Trifu, C.-I., Urbancic, T.I., 1996. Fracture coalescence as a mech-

anism for earthquakes: Observations based on mining induced microseismicity. Tectonophysics 261, 193–207.

Urbancic, T.I., Young, R.P., 1993. Space–time variations in source parameters of mining-induced seismic events with $M < 0$. Bull. Seismol. Soc. Am. 83, 378–397.

Urbancic, T.I., Trifu, C.-I., Young, R.P., 1993. Microseismicity derived fault-planes and their relationship to focal mechanism, stress inversion, and geologic data. Geophys. Res. Lett. 20, 2475–2478.

Urbancic, T.I., Trifu, C.-I., Shumila, V., 1997. Investigating the extent of excavation influence using deformation state analysis. In: Gibowicz, S.J. (Ed.), Rockbursts and Seismicity in Mines. A.A. Balkema, Rotterdam, Netherlands, pp. 185–189.